

# The stability of stratified, rotating systems and the generation of vorticity in the Sun

Steven A. Balbus<sup>1,2,3</sup>, Emmanuel Schaan<sup>1,3</sup>

## ABSTRACT

We examine the linear behavior of three-dimensional Lagrangian displacements in a stratified, shearing background. The isentropic and iso-rotation surfaces of the equilibrium flow are assumed to be axisymmetric, but otherwise fully two-dimensional. Three-dimensional magnetic fields are included in the perturbation equations; however the equilibrium is assumed to be well-described by purely hydrodynamic forces. The model, in principle very general, is used to study the behavior of fluid displacements in an environment resembling the solar convection zone. Some very suggestive results emerge. All but high-latitude displacements align themselves with the observed surfaces of constant angular velocity. The tendency for the angular velocity to remain constant with depth in the bulk of the convective zone, together with other critical features of the rotation profile, emerge from little more than a visual inspection of the governing equation. In the absence of a background axial angular velocity gradient, displacements exhibit no poleward bias, suggesting that solar convection “plays-off” of preexisting shear rather than creates it. We argue that baroclinic vorticity of precisely the right order is generated at the radiative/convective zone boundary due to centrifugal distortion of equipotential surfaces that is not precisely followed by isothermal surfaces. If so, many features of the Sun’s internal rotation become more clear, including: i) the general appearance of the tachocline; ii) the extension of differential rotation well into the radiative zone; iii) the abrupt change of morphology of convective zone isorotation surfaces; and iv) the inability of current numerical simulations to reproduce the solar rotation profile without imposed entropy boundary conditions.

---

<sup>1</sup>Laboratoire de Radioastronomie, École Normale Supérieure, 24 rue Lhomond, 75231 Paris CEDEX 05, France [steven.balbus@lra.ens.fr](mailto:steven.balbus@lra.ens.fr)

<sup>2</sup>Institut universitaire de France, Maison des Universités, 103 blvd. Saint-Michel, 75005 Paris, France

<sup>3</sup>Department of Astrophysical Sciences, Peyton Hall, Princeton University, Princeton NJ 08544, USA

*Subject headings:* convection — hydrodynamics — Sun: helioseismology — Sun: rotation

## 1. Introduction

In its most general form, the dynamical state of the interior of a star is one of differential rotation and entropy stratification. If isobaric and isochoric surfaces do not coincide, the angular velocity need not be constant on cylinders. A notable example is the Sun, for which helioseismology studies have fashioned a remarkably detailed and rich portrait. Where the Sun is stably stratified in entropy, in the bulk of the radiative zone, it tends not to be differentially rotating. However, surrounding the radius of vanishing entropy gradient, in both the convective *and* radiative layers, there is significant differential rotation generally dominated by the radial component of the angular velocity gradient. Higher in the convection zone, the rotation contours show an abrupt change in morphology, with the sudden emergence of a distinctly conical pattern (e.g. Miesch & Toomre 2009). Finally, approaching the Sun’s surface, there is once again an abrupt shift in contour morphology, apparently associated with the onset of high-velocity convection.

In previous work (Balbus, Latter, & Weiss 2012 [BLW] and references therein), it has been shown that the pattern of coaxial cones in the bulk of the solar convective zone (SCZ) can be understood as an elementary solution of the vorticity equation (in the limit of thermal wind balance) under certain well-posed assumptions. One of these assumptions is that a small angular entropy gradient is present, for without this there can be no axial component of the angular velocity gradient. Where does this all-important entropy gradient come from? Is it, as is often argued, an ineluctable consequence of convection and the Coriolis force, or is something more—or something else—involved? For that matter, is the entropy gradient more or less fundamental than the concomitant angular velocity gradient?

To address these questions, we begin with a very general study of the linear behavior of three-dimensional fluid displacements in a shearing and stratified background medium. The background angular velocity and entropy profiles may depend upon both poloidal coordinates. It is demonstrated that for a medium in uniform rotation, the most unstable displacements do *not* deflect from spherically radial paths, despite the presence of Coriolis forces. When an axial component of the angular velocity gradient is *already* present however, it is shown that there is a significant polar deflection of higher entropy fluid elements. More precisely, the sense of this deflection is poleward for outward-moving displacements if the axial angular velocity gradient is negative (as in the Sun), and *equatorial* if this gradient is positive. Thus, an axial angular velocity gradient is self-reinforcing, and may thus be

reshaped, in a convective fluid. Angular velocity gradients in cylindrical radius are much less effective in this regard: they have no first order effect on convective displacements. Because a background axial angular velocity gradient requires a vorticity source, this has far reaching consequences, and we use this finding as a thin edge of wedge to pry further into the origins of the Sun’s baroclinic differential rotation. We argue in particular that it is likely that the rotation pattern of the SCZ has emerged by responding to a preexisting angular entropy gradient, rather than generating such a gradient internally. This is entirely consistent with the experience of numerical simulations, in which rotation on cylinders stubbornly persists unless latitudinal entropy boundary conditions are present, in which case solar-like profiles emerge relatively easily (e.g. Miesch, Brun, Toomre 2006). Indeed, if the conclusions of this paper are well-founded, the direct imposition of such boundary conditions is the “correct” procedure!

In the second part of this paper, we put forth the case that vorticity generation is all but inevitable near the outer edge of the radiative zone where the entropy gradient vanishes. The combination of diffusive heating and centrifugal distortion of equipotential surfaces is incompatible with radiative and dynamical equilibrium in a uniformly rotating medium. The classic remedy of introducing a tiny amount of meridional circulation (e.g., Schwarzschild 1958) breaks down at a surface of zero entropy gradient. Instead, radiative equilibrium is re-established with very slightly different isothermal and isochoric surfaces. If, as one would expect from radiative considerations, the isotherms are more spherical than the isochoric surfaces, an incipient tachocline is generated, bearing many of the features observed of the true solar tachocline: a negative axial gradient of the angular velocity everywhere, a dominant (spherical) radial component of this gradient, and an increasingly dominant cylindrical disposition of the isorotation contours toward the equator.

The generation of vorticity at a level stemming from the centrifugal distortion of the equipotential surfaces has not been hitherto viewed as an important component of the solar differential rotation profile. However, not only is the centrifugal distortion of precisely the correct order-of-magnitude for this problem, we argue that it is the principal causal agent. If this is correct, numerical simulations whose goal is to reproduce the Sun’s internal rotation accurately from first principles will ultimately have to accomodate this  $1 : 10^5$  effect.

The organization of the paper is as follows. In §2, we present the governing equations for three-dimensional fluid displacements in an axisymmetric but otherwise fully general entropy-stratified, shearing background. This is an interesting gasdynamical problem in its own right, and particularly relevant for the sun. General solutions are presented in §3, but we focus on the most rapidly growing modes, for which a simple analysis is possible. The solution shows explicitly the relationship between shear, Coriolis forces, and the deflection of

convective trajectories. In §4, we integrate our findings with standard solar models, arguing that the seed angular entropy gradient is a result of centrifugal distortion of equipotential surfaces in the radiative zone together with the disappearance of the entropy gradient at the SCZ boundary. Finally, §5 summarizes our results.

## 2. Linear convection theory: fundamental equations

### 2.1. Equilibrium state

Throughout this paper, we use standard cylindrical coordinates (with  $R$  the radial distance from the rotation axis,  $\phi$  the azimuthal angle, and  $z$  the distance along the rotation axis) and standard spherical coordinates (with  $r$  the radial distance from the origin,  $\theta$  the colatitude angle from the  $z$  axis, and  $\phi$  the azimuthal angle). Unit vectors will be denoted by an appropriately subscripted  $\mathbf{e}$ .

The unperturbed background state is one of time-steady hydrostatic equilibrium,

$$R\Omega^2 \mathbf{e}_R = \frac{1}{\rho} \nabla P + \nabla \Phi \quad (1)$$

Here,  $\Omega$  is the angular velocity,  $\rho$  the mass density,  $P$  the gas pressure, and  $\Phi$  the gravitational potential. The magnetic field  $\mathbf{B}$  is assumed to be weak and may be ignored in the equilibrium state, but large wavenumber perturbations could in principle be significantly influenced by the field. We therefore will retain the magnetic field when analyzing small disturbances. Equation (1) is quite general for hydrostatic stars or disks, but for SCZ applications it is an excellent approximation to take  $\Phi = -GM_\odot/r$  ( $G$  is the Newtonian constant and  $M_\odot$  is one solar mass), and to ignore the centrifugal force in the equilibrium state.

The centrifugal term can of course never be ignored in the vorticity equation (the  $\phi$  component of the curl of equation [1]), which provides a measure of the departure of isobaric and isochoric surfaces:

$$R \frac{\partial \Omega^2}{\partial z} = \frac{1}{\rho^2} \left( \frac{\partial \rho}{\partial R} \frac{\partial P}{\partial z} - \frac{\partial \rho}{\partial z} \frac{\partial P}{\partial R} \right), \quad (2)$$

which may also be written

$$R \frac{\partial \Omega^2}{\partial z} = \frac{1}{\gamma \rho} \left( \frac{\partial \sigma}{\partial z} \frac{\partial P}{\partial R} - \frac{\partial \sigma}{\partial R} \frac{\partial P}{\partial z} \right) \quad (3)$$

where  $\gamma$  is the adiabatic index, and  $\sigma \equiv \ln P \rho^{-\gamma}$  is proportional to the specific entropy. The right side of (3) may be written in spherical coordinates as

$$R \frac{\partial \Omega^2}{\partial z} = \frac{1}{r\gamma\rho} \left( \frac{\partial \sigma}{\partial r} \frac{\partial P}{\partial \theta} - \frac{\partial \sigma}{\partial \theta} \frac{\partial P}{\partial r} \right) \simeq \frac{g}{r\gamma} \frac{\partial \sigma}{\partial \theta} \quad (\text{SCZ approximation}) \quad (4)$$

where  $g = -(1/\rho)(\partial P/\partial r)$  is an excellent approximation to the gravitational acceleration, and the final approximate equality assumes that the radial component of the entropy gradient does *not* exceed the latitudinal component by many orders of magnitude. Equation (4), often referred to as the thermal wind equation (e.g. Pedlosky 1987), appears to be well satisfied throughout much of the SCZ.

## 2.2. Inertial terms

To understand more fully the complex dynamics of the SCZ, we analyze here a much simpler proxy system: the local linear behavior of three-dimensional linear disturbances in weakly magnetized, stratified, differentially rotating, two-dimensional background flows. Note that although the equilibrium is axisymmetric, the disturbances are fully three-dimensional. Our focus is the temporal behavior of the fluid displacements embedded in such a medium.

Nonlinear convection generally involves coherent, extended structures. A local WKB treatment cannot hope to capture fully this element of the problem. Instead, by affording some insight as to how uniformly rotating surfaces arise and host convective displacements, the local theory can suggest the origin of structure on larger scales. Such structure is able to survive despite the presence of shear.

The fundamental dynamical equation of motion for the linear perturbations is

$$\frac{\partial \mathbf{v}}{\partial t} + (\mathbf{v} \cdot \nabla) \mathbf{v} + \frac{1}{\rho} \nabla \left( P + \frac{B^2}{8\pi} \right) + \nabla \Phi - \frac{(\mathbf{B} \cdot \nabla) \mathbf{B}}{4\pi\rho} = 0. \quad (5)$$

As noted, while the magnetic field  $\mathbf{B}$  is assumed to play no role in the equilibrium state, it can still be important for the evolution of large wavenumber perturbations, and will be retained. We wish to explore the nonaxisymmetric behavior of local disturbances. Because the background flow is in a state of differential rotation, we work in a locally shearing Lagrangian coordinate system, and the linear perturbations are ultimately to be expressed in terms of the Lagrangian fluid element displacement  $\boldsymbol{\xi}(R, \phi, z, t)$ .

Begin by taking standard Eulerian perturbations ( $\delta \mathbf{v}$ ,  $\delta P$ , etc.) of the usual fluid equations. The linearized equation of motion is

$$\frac{D}{Dt} \delta \mathbf{v} + (\delta \mathbf{v} \cdot \nabla) \mathbf{v} - \frac{\delta \rho}{\rho^2} \nabla P + \frac{\nabla}{\rho} \left( \delta P + \frac{\mathbf{B} \cdot \delta \mathbf{B}}{4\pi} \right) - \frac{(\mathbf{B} \cdot \nabla) \delta \mathbf{B}}{4\pi\rho} = 0, \quad (6)$$

where

$$\frac{D}{Dt} = \frac{\partial}{\partial t} + \Omega \frac{\partial}{\partial \phi} \quad (7)$$

is the Lagrangian time derivative associated with the unperturbed flow. The magnetic pressure buoyancy term and the magnetic tension term involving the gradient of the background magnetic field have been dropped under the assumption that the field is weak. We make the standard WKB assumption that the product of the perturbation wavenumber with any background scale height is large.

Consider the first two terms of equation (6),

$$\frac{D}{Dt}\delta\mathbf{v} + (\delta\mathbf{v}\cdot\nabla)\mathbf{v} \equiv \frac{\partial\delta\mathbf{v}}{\partial t} + \Omega\frac{\partial\delta\mathbf{v}}{\partial\phi} + (\delta\mathbf{v}\cdot\nabla)(R\Omega\mathbf{e}_\phi) \quad (8)$$

The  $R$  and  $\phi$  components of these terms are, respectively,

$$\mathbf{e}_R\cdot\left[\frac{D}{Dt}\delta\mathbf{v} + (\delta\mathbf{v}\cdot\nabla)\mathbf{v}\right] = \frac{D\delta v_R}{Dt} - 2\Omega\delta v_\phi, \quad (9)$$

$$\mathbf{e}_\phi\cdot\left[\frac{D}{Dt}\delta\mathbf{v} + (\delta\mathbf{v}\cdot\nabla)\mathbf{v}\right] = \frac{D\delta v_\phi}{Dt} + \frac{\kappa^2}{2\Omega}\delta v_R + R\left(\frac{\partial\Omega}{\partial z}\right)\delta v_z, \quad (10)$$

where

$$\kappa^2 = 2\Omega\left[\Omega + \frac{\partial(R\Omega)}{\partial R}\right]. \quad (11)$$

The  $z$  component is simply

$$\mathbf{e}_z\cdot\left[\frac{D}{Dt}\delta\mathbf{v} + (\delta\mathbf{v}\cdot\nabla)\mathbf{v}\right] = \frac{D\delta v_z}{Dt}. \quad (12)$$

The relationship between  $\boldsymbol{\xi}$  and  $\delta\mathbf{v}$  is given by

$$\frac{D\boldsymbol{\xi}}{Dt} = \delta\mathbf{v} + \boldsymbol{\xi}\cdot\nabla(R\Omega\mathbf{e}_\phi) \quad (13)$$

For  $j$  equal to  $R$  or  $z$ , we find  $\delta v_j = D\xi_j/Dt$ , while the  $\phi$  component of (13) gives

$$\frac{D\xi_\phi}{Dt} = \delta v_\phi + R(\boldsymbol{\xi}\cdot\nabla)\Omega \quad (14)$$

Equations (9) and (10) may now be expressed in terms of  $\xi_R$  and  $\xi_\phi$ , becoming respectively

$$\mathbf{e}_R\cdot\left[\frac{D}{Dt}\delta\mathbf{v} + (\delta\mathbf{v}\cdot\nabla)\mathbf{v}\right] = \ddot{\xi}_R - 2\Omega\dot{\xi}_\phi + R(\boldsymbol{\xi}\cdot\nabla)\Omega^2, \quad (15)$$

$$\mathbf{e}_\phi\cdot\left[\frac{D}{Dt}\delta\mathbf{v} + (\delta\mathbf{v}\cdot\nabla)\mathbf{v}\right] = \ddot{\xi}_\phi + 2\Omega\dot{\xi}_R, \quad (16)$$

where the dot notation indicates the Lagrangian derivative  $D/Dt$ . Putting the last two equations together with the  $z$  equation of motion leads to the vector equation

$$\frac{D}{Dt}\delta\mathbf{v} + (\delta\mathbf{v}\cdot\nabla)\mathbf{v} = \ddot{\boldsymbol{\xi}} + 2\boldsymbol{\Omega} \times \dot{\boldsymbol{\xi}} + \mathbf{e}_R R(\boldsymbol{\xi}\cdot\nabla)\Omega^2 \quad (17)$$

The second term on the right is obviously the Coriolis term, and the final term is the “residual centrifugal force:” the difference between the centrifugal force in the rotating frame and the forces maintaining the differential rotation. Notice the appearance of  $\nabla\Omega^2$ , as opposed to an angular momentum gradient, as part of the inertial forces.

### 2.3. Linear perturbations: magnetic induction and entropy constraints

Next, recall the relationship between  $\delta\mathbf{B}$  and the displacement  $\boldsymbol{\xi}$ , which follows from the integrated form of the induction equation,

$$\delta\mathbf{B} = \nabla \times (\boldsymbol{\xi} \times \mathbf{B}) \quad (18)$$

We work in the Boussinesq limit,

$$\nabla \cdot \boldsymbol{\xi} = 0, \quad (19)$$

so that equation (18) becomes

$$\delta\mathbf{B} = (\mathbf{B}\cdot\nabla)\boldsymbol{\xi}. \quad (20)$$

We have dropped the term  $(\boldsymbol{\xi}\cdot\nabla)\mathbf{B}$  under the WKB assumption that the displacements are rapidly varying in space.

Finally, for adiabatic perturbations,

$$\gamma \frac{\delta\rho}{\rho} = \boldsymbol{\xi}\cdot\nabla\sigma, \quad (21)$$

since in the Boussinesq limit, the relative pressure perturbation  $\delta P/P$  is small compared with the relative density perturbation  $\delta\rho/\rho$ .

## 2.4. Comoving coordinates and wavenumbers

### 2.4.1. Time dependence of Eulerian wavenumbers

The final step is to transform to spatial Lagrangian coordinates comoving with the unperturbed flow, the “primed” coordinate system. This is accomplished by the transformation

$$R' = R, \quad \phi' = \phi - \Omega t, \quad z' = z, \quad t' = t, \quad (22)$$

where of course  $\Omega$  is a function of  $R$  and  $z$ . Use of the Lagrangian derivative  $D/Dt$  ( $\equiv \partial/\partial t'$ ) has already effected the transformation of the partial time derivative, and the two altered poloidal spatial derivatives are

$$\frac{\partial}{\partial R} = \frac{\partial}{\partial R'} - t \frac{\partial \Omega}{\partial R} \frac{\partial}{\partial \phi'}, \quad (23)$$

$$\frac{\partial}{\partial z} = \frac{\partial}{\partial z'} - t \frac{\partial \Omega}{\partial z} \frac{\partial}{\partial \phi'}. \quad (24)$$

More compactly,

$$\nabla = \nabla' - (t \nabla \Omega) \frac{\partial}{\partial \phi'}, \quad (25)$$

a relation that holds for all three components of the gradient. In the WKB limit, all disturbances in Lagrangian comoving coordinates have the spatial dependence

$$\exp [i (k'_R R' + m \phi' + k'_z z')] \quad (26)$$

in which all components of the  $\mathbf{k}'$  wave vector are constants. This means that the Eulerian spatial derivatives of  $R$  and  $z$  are replaced locally (and respectively) by  $ik_R(t)$  and  $ik_z(t)$ , where

$$k_R(t) = k'_R - mt \frac{\partial \Omega}{\partial R}, \quad (27)$$

$$k_z(t) = k'_z - mt \frac{\partial \Omega}{\partial z}. \quad (28)$$

Henceforth, the time dependence of  $k_R$  and  $k_z$  will be understood with

$$\dot{k}_R = -m \frac{\partial \Omega}{\partial R}, \quad \dot{k}_z = -m \frac{\partial \Omega}{\partial z}. \quad (29)$$

Note that for initially purely azimuthal  $e^{im\phi'}$  disturbances, the poloidal wavenumber components comprise a two-dimensional vector parallel to  $-\nabla \Omega$ .

#### 2.4.2. Lagrangian displacements and isorotation surfaces

At sufficiently large times  $t$  (or all times if  $k'_R = k'_z = 0$ ),

$$\frac{k_R}{k_z} \rightarrow \frac{\partial \Omega / \partial R}{\partial \Omega / \partial z} \quad (30)$$

and the wave vector becomes increasingly axisymmetric as the poloidal components grow. If the three components of the displacement  $\boldsymbol{\xi}$  are of comparable magnitude, then the condition  $\mathbf{k} \cdot \boldsymbol{\xi} = 0$  becomes, at sufficiently large  $t$ ,

$$\boldsymbol{\xi} \cdot \nabla \Omega = 0, \quad (31)$$

whence

$$\dot{\boldsymbol{\xi}} \cdot \nabla \Omega = 0. \quad (32)$$

In other words, *independently of the details of the dynamics*, the velocity vector of a disturbed fluid element must eventually lie in a surface of constant  $\Omega$ . There is nothing “solar” about this argument, it relies entirely on the kinematics of differential rotation and mass conservation in an incompressible fluid. But it is tempting to apply this to the Sun, since the fluid elements in question would then be convecting heat and eliminating excess entropy gradients within surfaces of constant  $\Omega$ , and the confluence of these surfaces with constant residual entropy surfaces becomes less mysterious. There is a further benefit to such an approach: the preponderance of the constant  $\Omega$  surfaces are *observed* to be quasi-radial spokes, as seen in meridional cross section. They are customarily if crudely described as cones of constant  $\theta$ . If the radially convecting elements are compelled to follow paths of constant  $\Omega$ , then  $\Omega \simeq \Omega(\theta)$  is hardly mysterious. (Precisely the same vanishing-divergence reasoning also leads to the conclusion that the poloidal components of the magnetic field vector should lie in constant  $\Omega$  surfaces.)

Is this kinematical argument for the alignment of constant residual entropy and angular velocity surfaces correct? This depends upon whether there is sufficient time for the shear to shape the wavelet before coherence is lost. A potential difficulty is that, as the differential rotation is not large, this may be a rather long time interval depending upon the initial poloidal wavenumber components. Long-lived, coherent, nonlinear and nonlocal structures are seen in fully-developed convection, and these will in fact tend to lie in constant  $\Omega$  surfaces. In some sense this backs our approach, but at the same time it puts the cart before the horse: it is just this rotation-entropy link we would like to understand. We suggest that a more rapid linear dynamical explanation is also available, whereby modes with very small initial poloidal wavenumbers and near radial displacements are preferred for rapid development. This is discussed in more detail in §2.6 and §3.

### 2.4.3. The constancy of $\mathbf{k} \cdot \mathbf{B}$

The  $\phi$  component of the equilibrium magnetic field is not independent of time, but satisfies the induction equation

$$\frac{\partial B_\phi}{\partial t} = R(\mathbf{B} \cdot \nabla)\Omega, \quad (33)$$

or

$$B_\phi = B'_\phi + tR(\mathbf{B} \cdot \nabla)\Omega. \quad (34)$$

Note, however, that the magnetic tension  $\mathbf{k} \cdot \mathbf{B} = \mathbf{k}' \cdot \mathbf{B}'$ , where  $\mathbf{B}'$  is the magnetic field at  $t = 0$ , is *independent of time*. Introducing the Alfvén velocity

$$\mathbf{v}_A \equiv \frac{\mathbf{B}}{\sqrt{4\pi\rho}}, \quad (35)$$

the quantity  $(\mathbf{k} \cdot \mathbf{v}_A)^2$ , the local magnetic tension force per unit mass, may be regarded as a locally constant parameter in the equations of motion.

## 2.5. Final Dynamical Equations

We may now assemble the three fundamental dynamical equations of motion:

$$\ddot{\xi}_R - 2\Omega\dot{\xi}_\phi + R(\boldsymbol{\xi} \cdot \nabla)\Omega^2 - \frac{\partial P}{\partial R} \frac{(\boldsymbol{\xi} \cdot \nabla)\sigma}{\gamma\rho} + ik_R \left( \frac{\delta P}{\rho} + \frac{\mathbf{B} \cdot \delta \mathbf{B}}{4\pi\rho} \right) + (\mathbf{k} \cdot \mathbf{v}_A)^2 \xi_R = 0, \quad (36)$$

$$\ddot{\xi}_\phi + 2\Omega\dot{\xi}_R + \frac{im}{R} \left( \frac{\delta P}{\rho} + \frac{\mathbf{B} \cdot \delta \mathbf{B}}{4\pi\rho} \right) + (\mathbf{k} \cdot \mathbf{v}_A)^2 \xi_\phi = 0, \quad (37)$$

$$\ddot{\xi}_z - \frac{\partial P}{\partial z} \frac{(\boldsymbol{\xi} \cdot \nabla)\sigma}{\gamma\rho} + ik_z \left( \frac{\delta P}{\rho} + \frac{\mathbf{B} \cdot \delta \mathbf{B}}{4\pi\rho} \right) + (\mathbf{k} \cdot \mathbf{v}_A)^2 \xi_z = 0. \quad (38)$$

The three dynamical equation may be combined into a single vectorial equation

$$\ddot{\boldsymbol{\xi}} + 2\boldsymbol{\Omega} \times \dot{\boldsymbol{\xi}} + \mathbf{e}_R R(\boldsymbol{\xi} \cdot \nabla)\Omega^2 - \frac{\nabla P}{\gamma\rho} \boldsymbol{\xi} \cdot \nabla \sigma + (\mathbf{k} \cdot \mathbf{v}_A)^2 \boldsymbol{\xi} + \frac{i\mathbf{k}}{\rho} \left( \delta P + \frac{\mathbf{B} \cdot \delta \mathbf{B}}{4\pi} \right) = 0 \quad (39)$$

with the understanding that  $\mathbf{k}$  in the final term is time dependent,

$$\mathbf{k}(t) = \mathbf{k}(0) - mt\nabla\Omega, \quad (40)$$

and

$$\mathbf{k}(t) \cdot \boldsymbol{\xi} = 0. \quad (41)$$

## 2.6. Self-consistent radial convection

It is a curious and significant fact that in the bulk of the convective zone the Sun tends to eliminate every extraneous *nonconvective* term in the linear equation (39), either by the term vanishing identically or by its cancellation with another nonconvective term. The dominant dynamics is due almost entirely to the underlying radial forcing from the unstable entropy gradient, even in the presence of rotation.

Recall the concept of residual entropy introduced by Balbus et al. (2009): the entropy  $\sigma(r, \theta)$  is written as the sum of a function depending only upon spherical radius,  $\sigma_r(r)$ , and a residual term,  $\sigma'(r, \theta)$ . Physically,  $\sigma_r$  represents the underlying convection-driving unstable radial entropy profile, and  $\sigma'$  is the  $\theta$ -dependent modification that results as a consequence of rotation plus convection. In numerical simulations, this breakdown has an operational significance:  $\sigma_r$  is externally imposed, and  $\sigma'$  is, in essence, the computed response (Miesch et al. 2006)<sup>1</sup>. Only  $\sigma'$  is relevant to the thermal wind equation (4), since the entropy appears exclusively in the form of  $\partial\sigma/\partial\theta$ .

We write  $\sigma = \sigma_r + \sigma'$  and let us assume that  $P$  is a function of  $r$  only. Then with  $g\mathbf{e}_r = -(1/\rho)\nabla P$ , the usual squared Brunt-Väisälä frequency  $N^2$  is

$$N^2 \equiv \frac{g}{\gamma} \frac{\partial\sigma}{\partial r} = \frac{g}{\gamma} \frac{\partial(\sigma_r + \sigma')}{\partial r} \equiv N_r^2 + \frac{g}{\gamma} \frac{\partial\sigma'}{\partial r}. \quad (42)$$

In the SCZ,  $N^2 < 0$ . Dropping the magnetic terms, as they appear to be genuinely tiny, equation (39) may then be written

$$\ddot{\boldsymbol{\xi}} + N_r^2 \xi_r \mathbf{e}_r + 2\boldsymbol{\Omega} \times \dot{\boldsymbol{\xi}} + \mathbf{e}_R R (\boldsymbol{\xi} \cdot \nabla) \Omega^2 - \frac{\nabla P}{\gamma \rho} \boldsymbol{\xi} \cdot \nabla \sigma' + \frac{i\mathbf{k}\delta P}{\rho} = 0 \quad (43)$$

Recall that the bulk of the SCZ is characterized by an angular velocity that is insensitive to depth; roughly speaking,  $\Omega \simeq \Omega(\theta)$ . Moreover, surfaces of constant  $\Omega$  and  $\sigma'$  coincide well (Miesch et al. 2006; Balbus et al. 2009). Under these circumstances, for the dominant radial  $\mathbf{e}_r$  convective displacements, *all terms in equation (43) vanish, cancel hydrostatically, or are otherwise negligible, save the first and second*. In particular, the Coriolis deflection (third term in from the left) is balanced by the azimuthal pressure gradient (final term on the left side), and the two  $\boldsymbol{\xi} \cdot \nabla$  terms are intrinsically small. The radially moving disturbances are characterized by poloidal wavenumber components very small compared with  $m/R$ . In other words, within the context of simple linear theory in a uniformly rotating sphere, we have a plausible beginning for understanding why the Sun’s gross pattern of *differential rotation* is the way it is: the most efficient way to convect heat outwards is by maintaining radial convection, which is however permitted only to the extent that the dynamical forces of differential rotation allow it. With  $\Omega = \Omega(\theta)$ , and fluid motions embedded within coinciding  $\Omega$  and  $\sigma'$  surfaces, the dynamics of radial convection in a shearing system is self-consistent. In fact, the data show that in the bulk of the SCZ, constant  $\Omega$  surfaces are slightly more axial than constant  $\theta$  surfaces. In the next section, we will see that poleward

---

<sup>1</sup>In practice, the computed  $\sigma'$  may acquire a purely spherical contribution as well, but this is easily removed by subtracting off the mean.

trajectory deviations emerge from the solutions of equation (43) when  $\partial\Omega/\partial z < 0$ . We shall argue, moreover, that these axial departures from radial trajectories furnish an important clue to the origin of the Sun’s vorticity.

## 2.7. Reduction to Two Coupled Equations

The equation of mass conservation  $\nabla \cdot \boldsymbol{\xi} = 0$  may be written

$$\xi_\phi = -\frac{R}{m} (k_R \xi_R + k_z \xi_z). \quad (44)$$

From this it follows

$$\dot{\xi}_\phi = -\frac{R}{m} (k_R \dot{\xi}_R + k_z \dot{\xi}_z) + R(\boldsymbol{\xi} \cdot \nabla)\Omega, \quad \ddot{\xi}_\phi = -\frac{R}{m} (k_R \ddot{\xi}_R + k_z \ddot{\xi}_z) + 2R(\dot{\boldsymbol{\xi}} \cdot \nabla)\Omega. \quad (45)$$

Next, from equation (38),

$$i \left( \frac{\delta P}{\rho} + \frac{\mathbf{B} \cdot \delta \mathbf{B}}{4\pi\rho} \right) = -\frac{1}{k_z} \left[ \ddot{\xi}_z + (\mathbf{k} \cdot \mathbf{v}_A)^2 \xi_z - \frac{\partial P}{\partial z} \frac{(\boldsymbol{\xi} \cdot \nabla)\sigma}{\gamma\rho} \right] \quad (46)$$

Substituting equations (44)- (46) into (36) and (37) and simplifying produces the equations

$$\ddot{\xi}_R + (\mathbf{k} \cdot \mathbf{v}_A)^2 \xi_R - \frac{k_R}{k_z} \left( \ddot{\xi}_z + (\mathbf{k} \cdot \mathbf{v}_A)^2 \xi_z \right) + \frac{2\Omega R}{m} (k_R \dot{\xi}_R + k_z \dot{\xi}_z) + \frac{\mathcal{D}P}{\rho\gamma} (\boldsymbol{\xi} \cdot \nabla)\sigma = 0, \quad (47)$$

$$\begin{aligned} \frac{Rk_R}{m} \left[ \ddot{\xi}_R + (\mathbf{k} \cdot \mathbf{v}_A)^2 \xi_R \right] + \left( \frac{Rk_z}{m} + \frac{m}{Rk_z} \right) \left[ \ddot{\xi}_z + (\mathbf{k} \cdot \mathbf{v}_A)^2 \xi_z \right] \\ - 2\dot{\boldsymbol{\xi}} \cdot \nabla(R\Omega) - \frac{m}{Rk_z\rho\gamma} \frac{\partial P}{\partial z} (\boldsymbol{\xi} \cdot \nabla)\sigma = 0, \end{aligned} \quad (48)$$

where (Balbus 1995):

$$\mathcal{D} = \left( \frac{k_R}{k_z} \frac{\partial}{\partial z} - \frac{\partial}{\partial R} \right) \quad (49)$$

Finally, we may recombine equations (47) and (48), separately isolating  $\ddot{\xi}_R$  and  $\ddot{\xi}_z$ :

$$\begin{aligned} \ddot{\xi}_R + (\mathbf{k} \cdot \mathbf{v}_A)^2 \xi_R - \frac{2mk_R}{Rk^2} \dot{\boldsymbol{\xi}} \cdot \nabla(R\Omega) + \frac{2\Omega R}{m} \frac{k_\perp^2}{k^2} (k_R \dot{\xi}_R + k_z \dot{\xi}_z) \\ + \frac{1}{\gamma\rho} (\boldsymbol{\xi} \cdot \nabla)\sigma \left( \frac{k_z^2}{k^2} \mathcal{D}P - \frac{m^2}{R^2 k^2} \frac{\partial P}{\partial R} \right) = 0, \end{aligned} \quad (50)$$

where  $k_{\perp}^2 = k_z^2 + m^2/R^2$ , and

$$\begin{aligned} \ddot{\xi}_z + (\mathbf{k} \cdot \mathbf{v}_A)^2 \xi_z - \frac{2mk_z}{Rk^2} \dot{\boldsymbol{\xi}} \cdot \nabla(R\Omega) - \frac{2\Omega R k_R k_z}{m k^2} (k_R \dot{\xi}_R + k_z \dot{\xi}_z) \\ - \frac{1}{\gamma\rho} (\boldsymbol{\xi} \cdot \nabla\sigma) \left( \frac{k_R k_z}{k^2} \mathcal{D}P + \frac{m^2}{R^2 k^2} \frac{\partial P}{\partial z} \right) = 0. \end{aligned} \quad (51)$$

Equations (50) and (51) are the fundamental coupled equations governing the behavior of Lagrangian displacements.

## 2.8. Plane wave limits: axisymmetry and uniform rotation

### 2.8.1. Axisymmetry

It is important to establish the axisymmetric behavior of the disturbances, since it represents the long time behavior of the nonaxisymmetric response. In particular, we have already noted that at large times the wavenumber ratio  $k_R/k_z$  is just the time-steady ratio of the corresponding  $\Omega$  gradients. By contrast,  $m$  remains fixed, so the mode becomes asymptotically axisymmetric as time increases and the poloidal wavenumbers grow. Thus, at late times *all* nonaxisymmetric modes behave as an axisymmetric mode whose value for  $\mathbf{k} \cdot \mathbf{v}_A$  is fixed but arbitrary, while the value for  $k_R/k_z$  is fixed by equation (30).

In the Appendix, the  $m \rightarrow 0$  limit of equations (50) and (51) is shown to lead to the dispersion relation of Balbus (1995):

$$\frac{k^2}{k_z^2} \varpi^4 + \varpi^2 \left[ \frac{1}{R^3} \mathcal{D}(R^4 \Omega^2) + \frac{1}{\rho\gamma} (\mathcal{D}P)(\mathcal{D}\sigma) \right] - 4\Omega^2 (\mathbf{k} \cdot \mathbf{v}_A)^2 = 0, \quad \varpi^2 = \omega^2 - (\mathbf{k} \cdot \mathbf{v}_A)^2. \quad (52)$$

or

$$\begin{aligned} \frac{k^2}{k_z^2} \omega^4 + \omega^2 \left[ \frac{1}{R^3} \mathcal{D}(R^4 \Omega^2) + \frac{1}{\rho\gamma} (\mathcal{D}P)(\mathcal{D}\sigma) - 2 \frac{k^2}{k_z^2} (\mathbf{k} \cdot \mathbf{v}_A)^2 \right] \\ + \frac{k^2}{k_z^2} (\mathbf{k} \cdot \mathbf{v}_A)^4 - (\mathbf{k} \cdot \mathbf{v}_A)^2 \left[ R \mathcal{D}\Omega^2 + \frac{1}{\rho\gamma} (\mathcal{D}P)(\mathcal{D}\sigma) \right] = 0 \end{aligned} \quad (53)$$

For applications to the SCZ, we are interested in the case in which the dominant balance of (53) is between the first two terms, and the magnetic terms are unimportant (Goldreich & Schubert 1967):

$$\frac{k^2}{k_z^2} \omega^2 + \frac{1}{R^3} \mathcal{D}(R^4 \Omega^2) + \frac{1}{\rho\gamma} (\mathcal{D}P)(\mathcal{D}\sigma) = 0 \quad (54)$$

With  $k_R/k_z = (\partial\Omega/\partial R)(\partial\Omega/\partial z)^{-1}$ , we find that

$$\mathcal{D}(R^4\Omega^2) = -4\Omega^2, \quad (55)$$

and<sup>2</sup>

$$\mathcal{D}P = \left(\frac{\partial\Omega}{\partial z}\right)^{-1} \left(\frac{\partial\Omega}{\partial R} \frac{\partial P}{\partial z} - \frac{\partial\Omega}{\partial z} \frac{\partial P}{\partial R}\right) = \left(\frac{\partial\Omega}{\partial z}\right)^{-1} (\nabla P \times \nabla\Omega) \cdot \mathbf{e}_\phi = \frac{\partial P}{\partial r} \left(\frac{\partial\Omega}{\partial z}\right)^{-1} \frac{1}{r} \frac{\partial\Omega}{\partial\theta}. \quad (56)$$

Hence, in terms of the gravitational field  $g = -(1/\rho)(\partial P/\partial r)$ ,

$$\frac{1}{\rho\gamma} \mathcal{D}P = -\frac{g}{\gamma r} \left(\frac{\partial\Omega}{\partial z}\right)^{-1} \frac{\partial\Omega}{\partial\theta}. \quad (57)$$

The right side of this equation consists of directly observed or easily calculated quantities. By similar reasoning,

$$\mathcal{D}\sigma = \mathcal{D}[\sigma_r(r) + \sigma'] = \frac{d\sigma_r(r)}{dr} \left(\frac{\partial\Omega}{\partial z}\right)^{-1} \frac{1}{r} \frac{\partial\Omega}{\partial\theta} \quad (58)$$

Here we have used the fact  $\mathcal{D}\sigma' = 0$ , since  $\sigma'$  shares isosurfaces with  $\Omega$ . Combining equations (54), (55), (57) and (58), we obtain

$$\omega^2 = |\nabla\Omega|^{-2} \left[ \left(\frac{\partial\Omega}{\partial z}\right)^2 4\Omega^2 + \left(\frac{\partial\Omega}{\partial\theta}\right)^2 \frac{g}{\gamma r^2} \frac{d\sigma_r}{dr} \right] \quad (59)$$

This dispersion relation is an interesting blend, melding a standard form for inertial/gravity waves in a *uniformly* rotating medium with  $\mathbf{k} \propto \nabla\Omega$  for the poloidal wavenumber components, which obviously requires the presence of differential rotation to be sensible. The dynamical effects of the rotational shear are lost ( $\mathcal{D}\Omega = 0$ ) when  $\mathbf{k}$  is parallel to  $\nabla\Omega$ .

For the interesting case of  $\Omega = \Omega(\theta)$ , the dispersion relation is

$$\omega^2 = 4\Omega^2 \sin^2 \theta + \frac{g}{\gamma} \frac{d\sigma_r}{dr} \quad (60)$$

In principle, these axisymmetric modes can be rotationally stabilized at equatorial or possibly significantly higher latitudes, depending on how the adverse radial entropy gradient is modeled. If present, this stabilization is of some practical importance in models in which the Sun is convecting in surfaces of constant  $\Omega$ : these asymmetric modes are *not* unstable. Non-axisymmetry is more than a complication, it is crucial to the convection process itself.

---

<sup>2</sup>The  $R$  partial derivative is of course always taken with  $z$  constant, and vice-versa; the  $r$  and  $\theta$  partial derivatives bear a similar relationship.

### 2.8.2. Uniform rotation limit

The dispersion relation for nonaxisymmetric plane waves in the limiting case of a uniformly rotating medium may be derived from equations (50) and (51):

$$\varpi^4 + \varpi^2 \left[ \left( \frac{1}{\rho\gamma} \mathcal{D}P \mathcal{D}\sigma - 4\Omega^2 \right) \frac{k_z^2}{k^2} + \frac{m^2}{k^2 R^2 \gamma \rho} \nabla P \cdot \nabla \sigma \right] - 4 \frac{k_z^2}{k^2} \Omega^2 (\mathbf{k} \cdot \mathbf{v}_A)^2 = 0 \quad (61)$$

where  $\varpi^2$  is defined in equation (52). Restricting the discussion to the nonmagnetic subcase, the dispersion relation becomes (Cowling 1951):

$$\omega^2 + \left[ \left( \frac{1}{\rho\gamma} \mathcal{D}P \mathcal{D}\sigma - 4\Omega^2 \right) \frac{k_z^2}{k^2} + \frac{m^2}{k^2 R^2 \gamma \rho} \nabla P \cdot \nabla \sigma \right] = 0. \quad (62)$$

Notice that  $m$  introduces its own form of coupling to the entropy gradients. Moreover, it is possible to eliminate rotation-induced moderating influences on the growth rate by first setting  $k_z = 0$ , and then to maximize this rate by setting  $k_R = 0$ . The maximum growth rate is the magnitude of the Brunt-Väisälä frequency  $|N|$ , corresponding to precisely radial  $r$  displacements. The pure  $m$  modes are more unstable than are modes contaminated by poloidal wavenumber components.

How is it possible for an element to move along a spherical radius in a rotating system without encountering Coriolis deflections? The answer, as noted earlier, is by striking a geostrophic balance<sup>3</sup> of the azimuthal forces:

$$2\rho R|N|\Omega\xi_R = -im\delta P \quad (63)$$

With  $k_r = k_\theta = 0$ , there are neither components of the Coriolis force in the  $\mathbf{e}_\theta$  or  $\mathbf{e}_r$  directions, nor are there unbalanced pressure gradient forces. The convective rolls occur preferentially in planforms of latitudinal arcs: the familiar “banana cells” often seen in laboratory experiments and simulations (e.g., Hart et al. 1986). Rotational forces have no effect on these rapidly growing linear disturbances, and therefore no effect on the convective stability criterion. If the squared Brunt-Väisälä frequency is negative, no amount of (uniform) rotation can stabilize modes with vanishing poloidal wavenumber components.

### 2.8.3. Differential rotation: leading order effects

The full problem of the evolution of three-dimensional disturbances in a two-dimensional background medium is a matter of some complexity, which we defer to the next section. But

---

<sup>3</sup>Perhaps “heliostrophic” is a more apt description for the problem at hand.

for applications to the SCZ,  $|r\nabla\ln\Omega| \sim 0.1$ , and it is appropriate to use this as a small parameter as a means to calculate and understand the leading order effects. If we take  $k_R = k_z = 0$  as the zeroth order solution, then the poloidal wavevector  $\mathbf{k}_p$  is (to all higher orders, in fact):

$$\mathbf{k}_p = -mt\nabla\Omega. \quad (64)$$

Expanding equations (50) and (51) to linear order in the  $\Omega$  gradients, we obtain two very simple equations:

$$\ddot{\xi}_R - R\frac{\partial\Omega^2}{\partial z}t\dot{\xi}_z - \frac{1}{\gamma\rho}\frac{\partial P}{\partial R}(\boldsymbol{\xi} \cdot \nabla)\sigma = 0. \quad (65)$$

$$\ddot{\xi}_z + R\frac{\partial\Omega^2}{\partial z}t\dot{\xi}_R - \frac{1}{\gamma\rho}\frac{\partial P}{\partial z}(\boldsymbol{\xi} \cdot \nabla)\sigma = 0. \quad (66)$$

To derive equations (65) and (66), note that terms linear in  $\partial\Omega^2/\partial z$  come from the third and fourth terms in equation (50), and from the third term in equation (51). In the former case, there is a cancellation of the  $\dot{\xi}_R$  terms, leaving a lone contribution from  $\dot{\xi}_z$ . In the latter case, only the  $\dot{\xi}_R$  contribution is linear in the  $\Omega$  gradient. In the end, only one additional term arises in each of equations (65) and (66) from the differential rotation, and in each case only the axial gradient of  $\Omega^2$  enters: if the rotation is constant on cylinders ( $\Omega = \Omega(R)$ ), there is *no* leading order (linear in the  $\Omega$  gradient) correction to the convective displacements. In other words, *baroclinic vorticity must be present in the background to obtain a deviation from radial motion at linear order in the differential rotation parameter.*

It is instructive to write (65) and (66) in terms of  $\xi_r$  and  $\xi_\theta$ , the (spherical) radial and colatitudinal displacements. If  $P \simeq P(r)$ , then to first order, (65) and (66) combine to give

$$\ddot{\xi}_r + R\frac{\partial\Omega^2}{\partial z}t\dot{\xi}_\theta - \frac{1}{\gamma}\frac{\partial P}{\partial r}(\boldsymbol{\xi} \cdot \nabla)\sigma = 0, \quad (67)$$

$$\ddot{\xi}_\theta - R\frac{\partial\Omega^2}{\partial z}t\dot{\xi}_r = 0, \quad (68)$$

Equation (68) shows that the amplitude of  $\xi_\theta$  will be linear in  $\partial\Omega^2/\partial z$ . This means that in equation (67), all of the  $\xi_\theta$  terms will be *second order* in the  $\Omega^2$  gradient. Since we are working to linear order in the angular velocity gradient, our equations become

$$\ddot{\xi}_r + N^2\xi_r = 0, \quad (69)$$

$$\ddot{\xi}_\theta = \frac{g}{r\gamma}\frac{\partial\sigma}{\partial\theta}t\dot{\xi}_r \quad (70)$$

where in equation (70), we have used thermal wind balance (4) to substitute for  $R\partial\Omega^2/\partial z$ . To this order, there is no change in the behavior of the radial component of the displacement, while a poleward-increasing entropy profile produces poleward deflections of a radially

outward moving convective displacement (i.e., one that bears excess entropy). With  $|N|t$  of order unity, the angular deflections of convective displacements from linear theory are very similar in magnitude to the observed departures of the iso- $\Omega$  surfaces from constant  $\theta$  cones in the bulk of the SCZ. This, we suggest, is no coincidence: convection and its hallmark of constant residual entropy are both intimately associated with constant  $\Omega$  surfaces in the bulk of the SCZ (BLW), and a poleward deflection of the fluid elements is unavoidable when  $\partial\Omega/\partial z < 0$ . The interesting point, as we have earlier noted, is that it seems there must be an external source of vorticity in place to drive the deflections.

### 3. Numerical solutions

#### 3.1. Representative parameters

We next consider exact numerical solutions of equations (50) and (51). There are four important solar model parameters that need to be fixed: the two components of the  $\Omega$  gradient, and the two components of the  $\sigma$  (entropy) gradient. The  $\Omega$  gradient components at a particular location may be read directly from the helioseismology data. The term  $\partial\sigma/\partial\theta$  then follows from the assumption of thermal wind balance. Finally,  $\partial\sigma/\partial r$  is taken from a published benchmark solar model (Stix 2004). Typical values for the  $\Omega$  gradient at midlatitudes near  $r = 0.85R_\odot$  are (Christensen-Dalsgaard & Thompson 2007):

$$\frac{\partial \ln \Omega}{\partial \ln R} \simeq 0.24 \quad \frac{\partial \ln \Omega}{\partial \ln z} \simeq -0.12 \quad (71)$$

Thermal wind balance (i.e., vorticity conservation) then gives

$$\frac{\partial \sigma}{\partial \theta} \simeq -4 \times 10^{-6} \quad (72)$$

while a standard mixing length model (Stix 2004) gives:

$$\frac{\partial \sigma}{\partial \ln r} \simeq -2.3 \times 10^{-5} \quad (73)$$

Thus, for  $\Omega = 400\text{nHz}$ ,

$$4\Omega^2 \simeq 2.5 \times 10^{-11}\text{s}^{-2}, \quad \frac{g}{\gamma r} \frac{d\sigma_r}{d \ln r} \simeq -8.7 \times 10^{-12}\text{s}^{-2} \quad (74)$$

(In the context of our model, once the gradients of  $\Omega^2$  have been taken directly from the helioseismology results and the  $\theta$  derivative of  $\sigma'$  from thermal wind balance, the  $r$  derivative of  $\sigma'$  is uniquely determined from requiring counteraligned gradients of  $\Omega^2$  and  $\sigma'$ . Then, equation (73) is understood as the radial gradient of  $\sigma_r$ .) For the particular values in equations (71)–(74), at latitudes less than  $54^\circ$ , the axisymmetric displacement solutions of equation (60) are stable.

### 3.2. Results

We integrate equations (50) and (51) for a variety of different initial velocities and wavenumbers. Our strategy is to choose initial wavenumbers lying in the plane tangent to  $\mathbf{e}_r$ , with a random initial velocity direction (perpendicular to the wavenumber), and an initial displacement of zero. The ensuing trajectories are then followed.

When the angular velocity is uniform and free of shear, the results are very simple: all trajectories rapidly become radial, regardless of their initial condition. In agreement with our analytic treatment, after a brief initial transient, there is no equatorial or poleward deflection, even with the Coriolis force. On the other hand, when an angular velocity profile is used that has been modeled with the helioseismology data, there are  $\sim 10\%$  poleward deflections on time scales of a month or two, just as equations (69) and (70) would predict.

Fig. 1.— Meridional slices of the Sun ( $r = 0.8R_\odot$ ) at four different times (in units of  $2\pi/\Omega$ ) showing the relative orientation of the radial direction (dotted black line), entropy flux (solid lines), and isorotation surfaces (dotted red lines). Everywhere but at the highest latitudes, the entropy flux aligns itself with the isorotation surfaces within a typical mixing time. See text for further details.

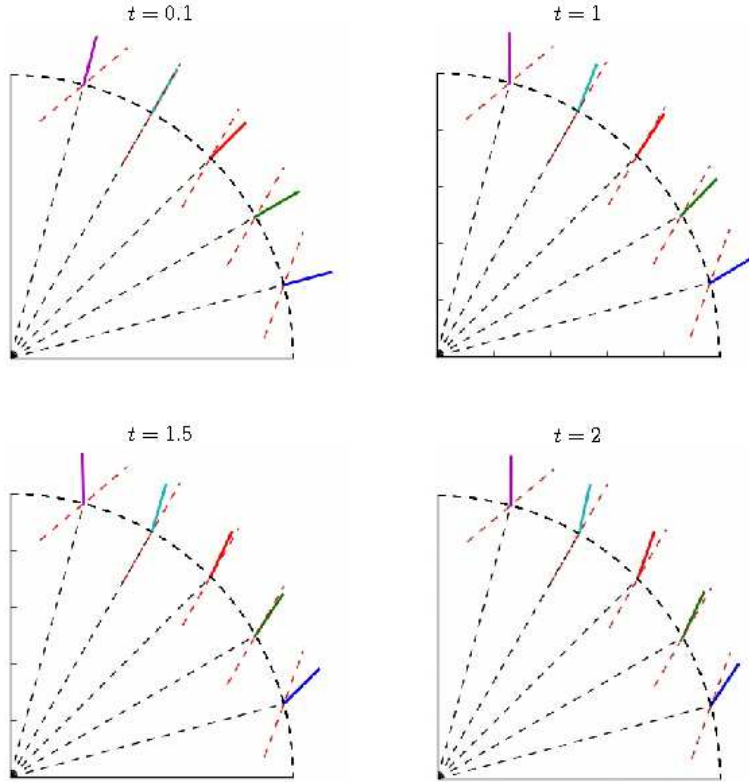


Figure (1) shows this effect clearly. We work at  $r = 0.8R_\odot$ , at latitudes  $15^\circ$ ,  $30^\circ$ ,  $45^\circ$ , and  $60^\circ$ . At each latitude, the surface of the local isorotation curve is shown, edge-on in a meridional plane, by a dotted red line. The local radial direction is shown by the black dotted line. The colored solid line at each latitude is the direction of the local *Eulerian* perturbation velocity, projected in the meridional plane. Four different times are shown. In each case, the trajectory passes through the local isorotational surface on a time scale of a few  $e$ -foldings, i.e. something close to a mixing time. Near the pole—above  $\sim 60^\circ$ —the trajectories begin and remain northward of the local isorotation surface, becoming more so with time. Here, the problem becomes close to one-dimensional, with all flow quantities predominantly a function of  $z$ . Our fundamental assumption that there is a functional relationship between angular velocity and residual entropy is then a matter of mathematical symmetry, not dynamics.

The torques required to maintain the fluid elements in or near surfaces of constant angular velocity are provided by azimuthal pressure gradients, as previously noted. *In no sense is the angular momentum of an individual fluid element conserved.* Consider however  $\delta v_\phi$ , the Eulerian perturbation of the angular velocity:

$$\delta v_\phi = \dot{\xi}_\phi - (R\dot{\xi} \cdot \nabla)\Omega = -R(k_r\dot{\xi}_r + k_\theta\dot{\xi}_\theta)/m, \quad (75)$$

where we have used equation (45) in the last equality, and switched to spherical coordinates. The wavenumber component  $k_r$  is very small in the bulk of the SCZ since it is proportional to  $\partial\Omega/\partial r$  and  $\Omega \simeq \Omega(\theta)$ . The term  $k_\theta\dot{\xi}_\theta$  term is quadratic in the  $\Omega$  gradients, thus also a very small quantity. Therefore, there is very little angular momentum transport propagated by the correlated fluctuation tensor component  $\dot{\xi}_r\delta v_\phi$ . Indeed, noting that if equation (64) holds for the poloidal wavenumber components, then

$$\delta v_\phi = -R(k_r\dot{\xi}_r + k_\theta\dot{\xi}_\theta)/m = Rt\dot{\xi} \cdot \nabla\Omega, \quad (76)$$

which for a near vanishing  $\delta v_\phi$  is a self-consistent indication that displacements do not stray from constant  $\Omega$  surfaces. Angular momentum could, in principle, still be directly advected by a nonvanishing poloidal mass flux, if one is present.

### 3.3. Linear convection theory: a summary

The linear behaviour of perturbations in a two-dimensional, stratified, differentially rotating medium is very different according to whether or not  $\Omega$  is dependent upon  $z$ . If  $\Omega$  depends only upon  $R$ , isobaric and isochoric surfaces coincide, there is no source of baroclinic vorticity, and the dominant convective displacements are radial. There is neither poleward nor equatorial bias in the heat transport. If  $\Omega$  depends upon  $z$ , isobaric and isochoric surfaces do not coincide, an explicit vorticity source is implicated, and outward moving, hotter

convective displacements deflect north or south depending upon whether  $\Omega$  respectively decreases or increases poleward.

The helioseismology data in the bulk of the SCZ are in accord with this description, with  $\partial\Omega^2/\partial z < 0$  and slightly upward cants to the constant  $\Omega$  surfaces. The question remains, however, of what the cause of this gradient is. Indeed, it is a classical case of begging the question: the fundamental angular entropy gradient, putatively arising from the interaction of rotation and convection, itself requires the preexistence of an axial  $\Omega$  gradient—the very gradient the angular entropy gradient is supposed to be explaining!

In the next section, we suggest a resolution to this problem.

## 4. Vorticity generation

### 4.1. Centrifugal distortion of stratified surfaces

It has long been known that a uniformly rotating star cannot simultaneously be both in radiative and hydrostatic equilibrium (e.g. Schwarzschild 1958). The difficulty is that the rotation induces centrifugal distortions of the isothermal surfaces—polar flattening and equatorial bulging—which are incompatible with a vanishing radiative flux divergence. The dimensionless number that sets the scale for these distortions is the centrifugal parameter, which for a (fictional) uniformly rotating Sun takes the value:

$$\epsilon_0 = \frac{R_\odot^3 \Omega^2}{GM_\odot} \sim 1.6 \times 10^{-5}. \quad (77)$$

(We have used  $\Omega = 2.5 \times 10^{-6}$ .) This is a very small number. But we are interested in entropy gradients of order

$$\frac{\partial\sigma}{\partial\theta} \sim 10^{-6}, \quad (78)$$

and it therefore behooves us to take note of centrifugally-induced angular gradients.

Normally, a tiny amount of meridional circulation is enough to offset the unbalanced radiative heating. Consider, however, conditions at the outer edge of the radiative zone. The entropy equation is

$$P \left[ \frac{\partial\sigma}{\partial t} + (\mathbf{v} \cdot \nabla)\sigma \right] = -(\gamma - 1)\nabla \cdot \mathbf{F}, \quad (79)$$

where  $\mathbf{F}$  is the radiative flux. If the divergence term on the right does not vanish at the radius where the entropy gradient does, there is no simple balance of the right and left sides of the equation. A balance could in principle be restored if a turbulent entropy flux divergence were

present, and this may indeed be representative of current conditions, but it is revealing to follow the breakdown of our simple uniform rotation model. Uneven heating would alter the flux until its divergence is minimized. (The time scale for this is simply the Kelvin-Helmholtz time;  $\epsilon_0$  is not involved.) This altered flux divergence will generally be incompatible with coincidence of isobaric and isochoric surfaces, which uniform rotation demands. We are thus led to the generation of differential rotation with an axial component of the angular velocity gradient (baroclinicity) to maintain thermal equilibrium. Even in a more complex setting with a thermal entropy flux divergence present, the base of the convective zone will follow the radiation flux divergence and almost certainly be more spherical than the equipotential surfaces. Once again baroclinic structure will be generated<sup>4</sup>.

The helioseismology data show unambiguously that the radius at which the entropy gradient vanishes is symmetrically placed within a narrow band of pronounced differential rotation: the tachocline. Moving from this radius downward into the radiative zone, uniform rotation takes over as the entropy gradient rises rapidly and meridional circulation is established. Moving upward into the convective zone, turbulent mixing quickly develops and there is an abrupt change of the character of the differential rotation: convective mixing leads at once to the coincidence of two important classes of surface, but not a coincidence that is compatible with uniform rotation. Rather, it is isorotational and residual entropy surfaces that now coincide. (Note the hidden but important role of nonaxisymmetry, as the convective modes are large  $m$  disturbances.) Turbulent convection, in this picture, does not generate “from scratch” the differential rotation in which it operates. Instead it reacts to, and reinforces, the angular velocity gradient bequeathed to it from the surface of vanishing entropy gradient. We suggest that this is a key ingredient to the organizational scheme of differential rotation in the Sun.

## 4.2. Octopolar structure

The centrifugal distortion of equipotential surfaces engendered by uniform rotation leaves temperature  $T$ , pressure  $P$  and density  $\rho$  functions of  $r[1 + \epsilon(r)P_2(\cos\theta)]$ , where  $P_2$  is the usual Legendre polynomial of second order, and  $\epsilon$  is a function only of radius  $r$  (of order  $\epsilon_0$ ). The function  $\epsilon$  is determined by solving the Poisson equation with appropriate boundary conditions (Schwarzschild 1958). At first glance it might be thought that the effect of vorticity generation and its differing iso-surfaces would be to create a distinct  $\epsilon$  for each structural variable:  $\epsilon_\rho(r)$ ,  $\epsilon_T(r)$ , etc. In fact, when vorticity is generated it is impossible

---

<sup>4</sup>We acknowledge the referee M. Miesch for emphasizing this point.

to satisfy basic rotational equilibrium without a  $P_4(\cos\theta)$  dependence in the *leading order* nonspherical structure of these variables.

The equation of rotational equilibrium is

$$R\Omega^2\mathbf{e}_R = \frac{1}{\rho}\nabla P + \nabla\Phi \quad (80)$$

where  $\Omega$  depends upon  $r$  and  $\theta$ . From the symmetry of our problem we would expect  $\Omega^2$  to be of the form

$$\Omega^2 = \Omega_0(r)^2 + q_2(r)P_2(\cos\theta) + q_4(r)P_4(\cos\theta) + \dots \quad (81)$$

where the  $q_{2i}$  are functions of  $r$  only. This is not necessarily an expansion in a small parameter, but for the region of interest the first two terms provide a very good approximation, with errors in  $\Omega^2 - \Omega_0^2$  about 10% very near the equator and less elsewhere<sup>5</sup>. The average of  $\Omega^2$  is the average of  $\Omega_0^2$  and will be denoted  $\overline{\Omega^2}$ . Then, we may write the force balance equation as

$$R(\Omega^2 - \overline{\Omega^2})\mathbf{e}_R = \frac{1}{\rho}\nabla P + \nabla\Phi' \quad (82)$$

where

$$\Phi' = \Phi - \frac{R^2}{2}\overline{\Omega^2} \quad (83)$$

Taking the divergence of equation (82),

$$\frac{1}{R}\frac{\partial}{\partial R}\left[R^2(\Omega^2 - \overline{\Omega^2})\right] = \nabla \cdot \left(\frac{1}{\rho}\nabla P\right) + 4\pi G\rho - 2\overline{\Omega^2} \quad (84)$$

or

$$\frac{1}{r}\left(\frac{\partial}{\partial r} + \frac{\cot\theta}{r}\frac{\partial}{\partial\theta}\right)\left[r^2\sin^2\theta(\Omega^2 - \overline{\Omega^2})\right] = \nabla \cdot \left(\frac{1}{\rho}\nabla P\right) + 4\pi G\rho - 2\overline{\Omega^2} \quad (85)$$

From the form of this equation, it is evident that if  $\Omega^2$  has terms through order  $P_l(\cos\theta)$  in its angular expansion, then  $\rho$  and  $P$  will in general have angular structure through  $P_{l+2}$  in the first order linear term of a small  $\epsilon_0$  expansion. Therefore, uniform rotation results in quadrupolar deformation of the iso-surfaces of all structural variables, whereas a simple  $\sin^2\theta$  latitudinal dependence of  $\Omega^2$  results in *octopolar* structure.

Consider a scenario in which the Sun is rotating uniformly. There are  $P_2$  distortions of iso-surfaces in the radiative zone, and no polar deflections of warm fluid elements in the convective zone. Baroclinic vorticity would then be produced at the radius of vanishing

---

<sup>5</sup> Numerical fits generally are quoted for  $\Omega$  rather than  $\Omega^2$ ; the latter turns out to have a simpler expansion near the tachocline boundary. See Gough [2007] for convenient parameterizations of  $\Omega$ .

entropy gradient. Were only  $P_2$  structure to remain, the only self-consistent solution for the angular velocity would be  $\Omega = \Omega(r)$ . However,  $\partial\Omega/\partial z < 0$  would now also be present, causing first order poleward deflections of warm convective elements.

These results are very suggestive, and offer at least a heuristic approach to understanding the Sun’s poleward decreasing angular velocity profile. If  $\partial\Omega^2/\partial z < 0$  is maintained through the tachocline into the bulk of the SCZ, in which convection largely eliminates the  $r$  gradients of  $\Omega$  and  $\sigma'$ , then  $\partial\Omega^2/\partial\theta$  must be positive. To justify these assumptions in detail, however, one would need to know how angular momentum is transported and deposited by secondary flows (Meisch et al. 2012), and what is relative importance of vorticity forcing by nonconservative forces versus inertial vorticity conservation. These considerations, whose detailed origin lies outside the the scope of the current work, regulate the the  $\theta$  dependence of the pressure, density, entropy, and ultimately the angular velocity.

### 4.3. Solution for $\Omega^2$

The above considerations suggest that we regard the  $\rho$  (for example) as a function of the quantity

$$r_\rho \equiv r[1 + \epsilon_\rho(r)f_\rho(\cos^2 \theta)], \quad (86)$$

and similarly for  $P$  and  $T$ . The  $f_i(\cos^2 \theta)$  functions are linear combinations of  $P_2$  and  $P_4$ , in general distinct for  $i = \rho, P, T$ . (Recall that in the numerical simulations described by Miesch et al. (2006),  $P_l$  angular structure in the *entropy* was included as a boundary condition at the base of the convection zone. By far the best solar fit included  $P_2$  and  $P_4$  terms in the angular structure of the entropy.) Expanding  $r_\rho$ ,

$$\rho(r_\rho) = \rho_0(r) + \delta\rho(r) + \epsilon_\rho(r)\frac{d\rho_0}{d\ln r}f_\rho(\cos^2 \theta) + \dots \quad (87)$$

where  $\rho_0$  is the nonrotating solution and  $\delta\rho = \rho(r) - \rho_0(r)$ . To leading order,

$$\frac{\partial\rho}{\partial r} = \frac{d\rho_0}{dr}, \quad \frac{\partial\rho}{\partial\theta} = -2 \cos \theta \sin \theta \epsilon_\rho(r) \frac{d\rho_0}{d\ln r} f'_\rho(\cos^2 \theta), \quad (88)$$

with similar results for  $P$  and  $T$ . The notation  $f'$  denotes a derivative with respect to  $\cos^2 \theta$ . The  $f'$  functions are thus a linear superposition of  $\cos^2 \theta$  (or if more convenient  $\sin^2 \theta$ ) plus a constant term.

With this development, the vorticity equation becomes

$$\frac{\partial\Omega^2}{\partial z} = 2 \cos \theta (\epsilon_P f'_P - \epsilon_\rho f'_\rho) \frac{1}{\rho_0 r} \frac{dP_0}{dr} \frac{d\ln \rho_0}{dr}. \quad (89)$$

The demands of radiative equilibrium will require isothermal surfaces to be more spherical (less distorted) than are isochoric surfaces, whose centrifugal deformations are less critical to the heat flux. The pressure, being a product of  $\rho$  and  $T$ , would thus also be closer to spherically stratified than  $\rho$  itself. A simple mathematical approximation that allows progress and respects the observational fundamentals is to assume that the  $f$  stratification functions are the same for each variable, but that the  $\epsilon$  functions differ in magnitude from one variable to the next:  $\epsilon_\rho > \epsilon_P > \epsilon_T$ . We will also ignore the spatial variation of the  $\epsilon$  within the tachocline boundary layer.

These considerations lead to a vorticity equation of the form

$$\frac{\partial \Omega^2}{\partial z} = \frac{A}{r^4} \cos \theta (\sin^2 \theta - \alpha) \quad (90)$$

where  $A$  (of order  $\epsilon_0 GM_\odot$ ) and  $\alpha$  (of order unity) are positive constants. We have assumed  $1/r^2$  gravitational field and a  $1/r$  dependence for  $d \ln \rho / dr$ . Signs have been chosen so that  $\partial \Omega^2 / \partial z$  is negative at non-equatorial latitudes, as indicated by the helioseismology data. Another way to write this equation is

$$\frac{\mathcal{D} \Omega^2}{\mathcal{D} r} = \frac{A}{r^4} (\sin^2 \theta - \alpha) \quad (91)$$

where the characteristic derivative  $\mathcal{D}/\mathcal{D}r$  is taken along the path

$$r^2 \sin^2 \theta = \text{Constant} \equiv r_0^2 \sin^2 \theta_0 \quad (92)$$

In this form, the equation is close to the tachocline equation (19) of BLW, which is “correct” (in the sense that it agrees extremely well with the data), but derived from a completely different point of view. The sole difference in the two formalisms is that the  $\mathcal{D}/\mathcal{D}r$  derivative of BLW is taken along the path

$$r^2 \sin^2 \theta = r_0^2 \sin^2 \theta_0 + \beta r_0^2 \left(1 - \frac{r_0}{r}\right) \quad (93)$$

where  $\beta$  is a number of order unity. This is the characteristic path associated with the SCZ isorotation contours.

How closely do the two approaches agree? If  $\Omega^2$  is a given function  $\Omega_0^2(r_0^2 \sin^2 \theta_0)$  at radius  $r = r_0$ , then the solution of (91) and (92) is

$$\Omega^2 = \Omega_0^2(r_0^2 \sin^2 \theta_0) + A \int_{r_0}^r \left( \frac{r_0^2 \sin^2 \theta_0}{r^6} - \frac{\alpha}{r^4} \right) dr \quad (94)$$

or

$$\Omega^2 = \Omega_0^2(r_0^2 \sin^2 \theta_0) + \frac{A \sin^2 \theta_0}{5r_0^3} \left(1 - \frac{r_0^5}{r^5}\right) - \frac{A\alpha}{3r_0^3} \left(1 - \frac{r_0^3}{r^3}\right) \quad (95)$$

Next assume that

$$\Omega_0^2 \equiv \Omega_1^2 + \Omega_2^2 \sin^2 \theta_0 \quad (96)$$

where  $\Omega_1^2$  and  $\Omega_2^2$  are positive constants. (Recall that this is an excellent approximation for the boundary of the tachocline.) Using equation (92) and solving for the isorotation curves leads to

$$\sin^2 \theta = \frac{r_0^2}{r^2} \left( \frac{\Delta + C\alpha F_3}{1 + CF_5} \right) \quad (97)$$

where

$$\Delta = (\Omega^2 - \Omega_1^2)/\Omega_2^2, \quad C = A/(\Omega_2^2 r_0^3), \quad F_j = (1/j)[1 - (r_0/r)^j] \quad (98)$$

Note that  $\Delta$  is numerically the same as  $\sin^2 \theta_0$ ;  $C$  is a number of order  $\epsilon_0 \times 1/\epsilon_0 \sim$  unity.

As can be seen in figure (2), which shows our solution (97) next to the precise fit of BLW, the essential features of our result are basically correct. We have embedded the tachocline solution inside the same convective envelope solution in both cases. The principal area of disagreement is the bifurcation zone, on one side of which the isorotation contours break toward the pole and on the other side toward the equator. This is clearly the region where a crude approximation of the right side of equation (89) is likely to be most inaccurate. Our approach to the tachocline structure makes it more clear why the BLW equation works so well. An uncertain approximation used by BLW was the extension of the same simple functional dependence between  $\sigma'$  and  $\Omega^2$  into the tachocline. But in the region of interest near the bifurcation point, the tachocline solution really does become a smooth extension of the SCZ (and the tachocline belies its name). Away from the bifurcation zone, the functional dependence hardly matters, as it affects only the subdominant  $\partial\Omega^2/\partial\theta$  term in the governing equation.

The main point that one should take away from this exercise is that the combination of direct vorticity forcing together with a proper reckoning of the octopolar distortions of the structural variables  $P$  and  $\rho$  caused by the centrifugal forces of even the simplest latitude-dependence of the angular velocity seem to be important components of the rotational profile of the tachocline.

## 5. Conclusions

The current work combines two very different types of calculation, linking the linear dynamics of the convective zone to the origins of solar differential rotation and vorticity. We begin with the second part first.

We have argued that the centrifugal distortion of equipotential surfaces combined with

demands of thermal equilibrium requires the cleaving of isobaric and isochoric surfaces, and is likely to be the underlying cause of the Sun’s differential rotation. Current numerical simulations are not designed to capture a process in which an order  $\epsilon_0 \sim 10^{-5}$  radiative effect is turned into relative angular velocity gradients of order 0.1. It may well be possible, however, to devise other computational schemes tailored to working with this point-of-view.

An important technical point is that the tachocline pressure and density (and therefore entropy) must have both  $P_2(\cos\theta)$  and  $P_4(\cos\theta)$  angular structure. Although this in itself is not a particularly new result, neither has it been widely appreciated, and we have exploited it in a rather novel manner. With  $P_4$  and  $P_2$  structure in place, not only may one understand the simple form of the vorticity equation in the tachocline, with reasonable approximations one may explicitly solve the equation. An important parameter of this equation, namely the precise angle at which  $\partial\Omega^2/\partial r$  changes sign, is probably determined by minimizing the torque on the radiative interior. Finally, it is interesting to note that Roxburgh (2001) calculated the Sun’s multipole moments using models based on helioseismic inversions. He found that the size of the octopole term  $J_4$  was comparable to the *change* in the quadrupole term  $J_2$  when differential rotation was included. This is what one would expect if differential rotation were *modifying*  $P_2$  and *creating*  $P_4$  angular structures.

In the first part of this paper, we have carried out a very general Lagrangian linear calculation of the fluid displacements in an arbitrary, magnetized, two-dimensional background, stratified in both  $R$  and  $z$  (or  $r$  and  $\theta$ ). Applied to conditions appropriate to the SCZ, in the absence of a background  $\partial\Omega/\partial z$  gradient, we find no poleward deflection of hot convective fluid elements. Such an effect is sometimes invoked to produce an angular entropy gradient which would in turn lead to differential rotation via thermal wind balance. Although there is nothing in our calculations that would prohibit the emergence of the required gradients in  $\Omega$  and  $z$  at nonlinear order in a turbulent fluid, it is some significance that the dominant leading order linear response is completely different depending upon whether  $\partial\Omega/\partial z$  is present or absent. When a finite  $\partial\Omega/\partial z$  is *a priori* present, there are reinforcing convective deflections: a negative axial  $\Omega$  gradient, in particular, engenders poleward deflections of warmer fluid elements, which via thermal wind balance strengthen and maintain this same  $\Omega$  gradient. The presence or absence of background baroclinic vorticity is thus mirrored in the leading behavior of convective displacements.

The actual generation of baroclinic vorticity may well lie outside the realm of convection dynamics. We propose that a vorticity source will inevitably appear at the location of a vanishing entropy gradient. In general, because of the effects centrifugal flattening, the constraints of thermal and dynamical equilibrium will force different iso-surfaces for density, temperature, and pressure. This must lead to an axial angular velocity gradient. By making

some simplifying but plausible approximations, one may calculate a time-steady solution of the vorticity equation for the angular velocity. This explicit solution yields a tachocline structure that certainly resembles the observations, and bears comparison with an earlier, more accurate, but also more phenomenological, calculation (BLW). With the onset of fully developed convection, surfaces of constant angular velocity and residual entropy coincide, and the character of the isorotation contours takes on the classical conical form well-known from helioseismology.

The strength of this view of the origin of solar differential is that it emerges from just a few rather simple and largely inevitable processes: the demands of thermal energy balance in a rotating system (which creates a baroclinic axial gradient of  $\Omega$  at the radiative/convective boundary), the kinematics of shear (which, via embedded wavenumbers, incorporates  $\Omega$  gradients into the response of the fluid displacements), and the linear dynamics of convection (which causes poleward displacements of entropy bearing fluid elements). While direct numerical simulation of this scenario is likely to be very challenging, it may well be possible to design a test-of-principle proxy system.

### Acknowledgments

Much of this work was carried out while SB was a Paczynski Visitor and ES a visiting student researcher in the Department of Astronomy at Princeton University. We are grateful to Profs. D. Spergel and J. Stone for generous support during this visit. This work has also benefitted by grants from the Institut universitaire de France and the Conseil Régional de l’Île de France, and especially benefitted from a very constructive critique by our referee M. Miesch. It is a pleasure to acknowledge helpful conversations with H. Latter, P. Lesaffre, E. Quataert, J. Stone and N. Weiss, and to thank G. Mirou for spotting a technical error in an earlier draft of this work.

### REFERENCES

- Balbus, S. A., 1995, *ApJ*, 453, 380
- Balbus, S. A., Bonart, J., Latter, H. N., Weiss, N. O., 2009, *MNRAS*, 400, 176
- Balbus, S. A., Hawley, J. F. 1994, *MNRAS*, 266, 769
- Balbus, S. A., Latter, H., Weiss, N., 2012, *MNRAS*, 420, 2457 (BLW)

- Christensen-Dalsgaard, J., Thompson, M. J., 2007, in *The Solar Tachocline*, eds. D. Hughes, R. Rosner, N. Weiss, (Cambridge University Press: Cambridge), p. 53
- Cowling, T. G., 1951, *ApJ*, 114, 272
- Goldreich, P., Schubert, G., 1967, *ApJ*, 150, 571
- Gough, D. O., 2007, in *The Solar Tachocline*, eds. D. Hughes, R. Rosner, N. Weiss (Cambridge: Cambridge University Press), p. 3
- Gough, D. O., McIntyre, M. E., 1998, *Nature* 394, 755
- Hart J. E., Toomre, J., Deane, A. E., Hurlburt, N. E., Glatzmaier, G. A., Fichtl, G. H., Leslie, F., Fowles, W. W., Gilman, P., 1986, *Science*, 234, 4772, 61
- Miesch, M. S., Brun, A. S., Toomre, J., 2006, *ApJ*, 641, 618
- Miesch, M. S., Toomre, J., 2009, *Ann. Rev. Fluid Mech.*, 41, 317
- Parfrey, K. P., Menou, K., 2007, *ApJ*, 667, L207
- Pedlosky, J., 1987, *Geophysical Fluid Dynamics*, (Springer-Verlag: New York)
- Roxburgh, I. W., 2001, *A&A*, 377, 688
- Schwarzschild, M. 1958, *Structure and Evolution of the Stars* (Dover: New York)
- Stix, M., 2004, *The Sun, an Introduction* (Springer-Verlag: Berlin)

## Appendix

To recover the axisymmetric limit of equations (50) and (51), we begin with their equivalent forms (47) and (48):

$$\ddot{\xi}_R + (\mathbf{k} \cdot \mathbf{v}_A)^2 \xi_R - \frac{k_R}{k_z} \left( \ddot{\xi}_z + (\mathbf{k} \cdot \mathbf{v}_A)^2 \xi_z \right) + \frac{2\Omega R}{m} \left( k_R \dot{\xi}_R + k_z \dot{\xi}_z \right) + \frac{DP}{\rho\gamma} (\boldsymbol{\xi} \cdot \nabla) \sigma = 0, \quad (99)$$

$$\frac{Rk_R}{m} \left[ \ddot{\xi}_R + (\mathbf{k} \cdot \mathbf{v}_A)^2 \xi_R \right] + \left( \frac{Rk_z}{m} + \frac{m}{Rk_z} \right) \left[ \ddot{\xi}_z + (\mathbf{k} \cdot \mathbf{v}_A)^2 \xi_z \right]$$

$$-2\dot{\boldsymbol{\xi}} \cdot \nabla(R\Omega) + \frac{m}{Rk_z\rho\gamma} \frac{\partial P}{\partial z} (\boldsymbol{\xi} \cdot \nabla)\sigma = 0, \quad (100)$$

In the axisymmetric  $m \rightarrow 0$  limit, equation (99) may be written

$$\frac{2\Omega R}{m} \left( k_R \dot{\xi}_R + k_z \dot{\xi}_z \right) + \frac{k^2}{k_z^2} \left[ \ddot{\xi}_R + (\mathbf{k} \cdot \mathbf{v}_A)^2 \xi_R \right] + \frac{\mathcal{D}P}{\rho\gamma} (\boldsymbol{\xi} \cdot \nabla)\sigma = 0, \quad (101)$$

In what follows, we will also require the twice differentiated form of this equation,

$$\frac{2\Omega R}{m} \left( k_R \xi_R^{iii} + k_z \xi_z^{iii} \right) - 2R\ddot{\boldsymbol{\xi}} \cdot \nabla\Omega^2 + \frac{k^2}{k_z^2} \left[ \xi_R^{iv} + (\mathbf{k} \cdot \mathbf{v}_A)^2 \ddot{\xi}_R \right] + \frac{\mathcal{D}P}{\rho\gamma} (\ddot{\boldsymbol{\xi}} \cdot \nabla)\sigma = 0, \quad (102)$$

where the notation *iii* and *iv* denotes three and four time differentiations, respectively. Only the leading order terms in a small  $m$  expansion have been retained.

Now, in the axisymmetric limit, equation (100) becomes

$$\frac{R}{m} \left( k_R \ddot{\xi}_R + k_z \ddot{\xi}_z \right) + (\mathbf{k} \cdot \mathbf{v}_A)^2 \frac{R}{m} \left( k_R \xi_R + k_z \xi_z \right) - 2\dot{\boldsymbol{\xi}} \cdot \nabla(R\Omega) = 0 \quad (103)$$

Differentiating once,

$$\frac{R}{m} \left( k_R \xi_R^{iii} + k_z \xi_z^{iii} \right) + (\mathbf{k} \cdot \mathbf{v}_A)^2 \frac{R}{m} \left( k_R \dot{\xi}_R + k_z \dot{\xi}_z \right) - R \left[ \ddot{\boldsymbol{\xi}} + (\mathbf{k} \cdot \mathbf{v}_A)^2 \boldsymbol{\xi} \right] \cdot \nabla\Omega - 2\ddot{\boldsymbol{\xi}} \cdot \nabla(R\Omega) = 0. \quad (104)$$

The axisymmetric dispersion relation now follows from substituting equations (101) and (102) for the  $1/m$  terms into equation (104), setting  $\xi_z = -k_R \xi_R / k_z$ , and replacing all time derivatives by  $-i\omega$ . (The sign is chosen so that a positive wavenumber has a positive phase velocity.) After algebraic simplification, the result is

$$\frac{k^2}{k_z^2} \varpi^4 + \varpi^2 \left[ \frac{1}{R^3} \mathcal{D}(R^4 \Omega^2) + \frac{1}{\rho\gamma} (\mathcal{D}P)(\mathcal{D}\sigma) \right] - 4\Omega^2 (\mathbf{k} \cdot \mathbf{v}_A)^2 = 0, \quad \varpi^2 = \omega^2 - (\mathbf{k} \cdot \mathbf{v}_A)^2, \quad (105)$$

where  $\mathcal{D}$  is defined in equation (49). This is in precise agreement with Balbus (1995).

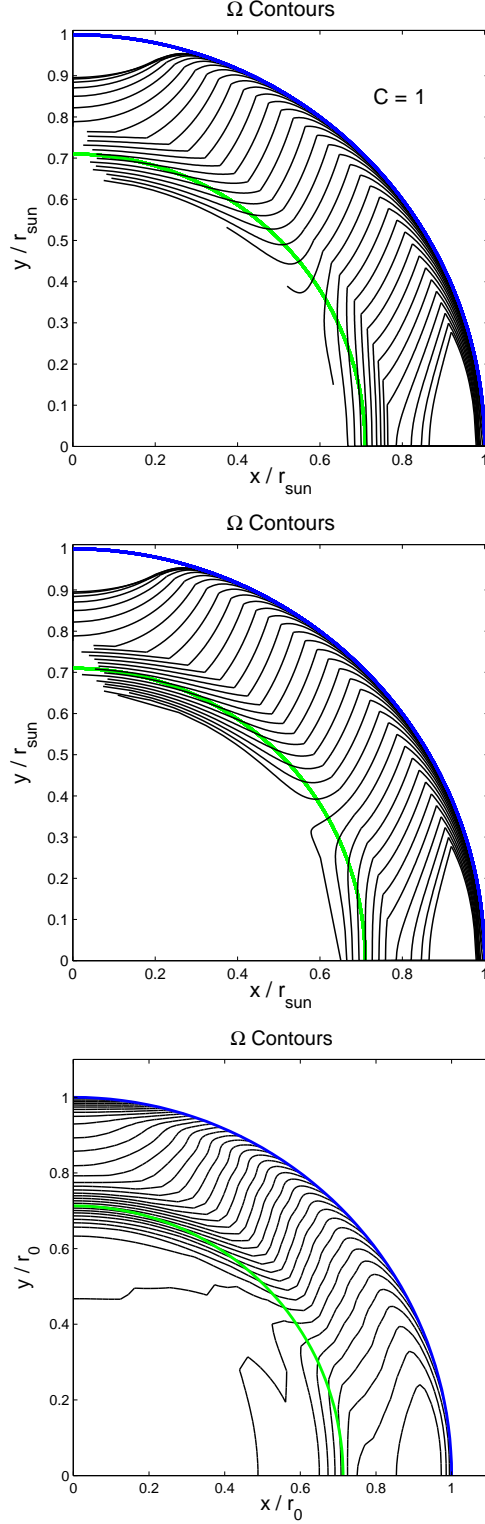


Fig. 2.— *Top:* The  $C = 1$ ,  $\alpha = 0.8$  tachocline solution of equation (91) along the trajectory characteristics of (92). Tachocline solutions are joined, at  $r = 0.77R_{\odot}$ , to the best fit solution of BLW for the SCZ and outer layers. Formal tachocline location is indicated by green line. *Middle:* The best fit global solution of BLW, in good agreement with observations. In this case, equation (91) is solved along characteristics given by (93). *Bottom:* GONG data, courtesy R. Howe.